Wind and Structures, Vol. 2, No. 4 (1999) 325-345
DOI: http://dx.doi.org/10.12989/was.1999.2.4.325

Prediction of pressure equalization performance of rainscreen walls

K. Suresh Kumar† and A.W.M. van Schijndel‡

Faculty of Architecture, Building and Planning, FAGO, Technical University of Eindhoven, Postbus 513, 5600 MB Eindhoven, The Netherlands

Abstract. In recent years, rainscreen walls based on the pressure equalization principle are often used in building construction. To improve the understanding of the influence of several design parameters on the pressure equalization performance of such wall systems, a theoretical consideration of the problem may be more appropriate. On this basis, this paper presents two theoretical models, one based on mass balance and the other based on the Helmholtz resonator theory, for the prediction of cavity pressure in rigid rainscreen walls. New measures to assess the degree of pressure equalization of rainscreen walls are also suggested. The results show that the model based on mass balance is sufficiently accurate and efficient in predicting the cavity pressure variations. Further, the performance of the proposed model is evaluated utilizing the data obtained from full-scale tests and the results are discussed in detail.

Key words: performance; prediction; pressure equalization; rainscreen walls.

1. Introduction

Pressure Equalized Rainscreen (PER) walls were developed to prevent or at least reduce rain penetration primarily caused by wind-induced pressure differentials across the wall. Essentially, this wall system incorporates two wall layers: an outer wall layer (rainscreen) and an inner wall layer (air barrier). The two wall layers are separated by a cavity that is vented to the exterior through openings on the rainscreen. These openings help to equalize the cavity pressure with the external wind pressure. The state-of-the-art information concerning the pressure equalized rainscreen approach to wall design has been documented elsewhere (Suresh Kumar 1998a, Suresh Kumar 2000). Although these wall systems were introduced about 3 decades ago, the existing design guidelines are more or less qualitative in nature. Furthermore, the pressure equalization phenomenon has been complicated by the influence of various parameters such as space and time varying external pressure, internal pressure, flexibility of the wall systems, volume of cavity, venting area (intended openings on the rainscreen) and leakage area (unintended openings on the air barrier). In these circumstances, it is of considerable interest to develop suitable analytical models for the efficient and cost effective parametric investigation of pressure equalization performance of rainscreen walls. Cavity pressure models and quantification methods are needed to

† Post Doctoral Fellow
‡ Lecturer

predict pressure equalization performance of rainscreen walls. In the past, very few studies have been carried out exclusively for the efficient prediction of pressure equalization performance of rigid rainscreen walls; therefore, further thoughts on this topic would be useful.

Within this context, this paper presents two different approaches for the theoretical prediction of cavity pressure in rigid rainscreen walls and suggests a suitable model. The paper also suggests methods to quantify the pressure equalization performance. For validation of the model, extensive comparisons have been performed using the data gathered from full-scale experiments. A few preliminary results of this study were reported in Suresh Kumar and van Schijndel (1998).

2. Previous work

The theoretical equation for cavity pressure is first introduced by Latta (1973) after assuming incompressible and orifice flow conditions. Later, Killip and Cheetham (1984) disputed this theory and suggested a new equation assuming that leakage paths through the air barrier are cracks instead of sharp edged orifices. In some studies (Fazio and Kontopidis 1988, Baskaran and Brown 1992), after assuming the domination of steady state incompressible flow conditions in the pressure equalization process, the volumetric rate flows into the cavity are equated to the volumetric rate flows out the cavity; the cavity pressure implicit in this formulation was solved iteratively. The extensive research on the prediction of internal building pressures over the last two decades can be extended to predict cavity pressures (Kerr 1985); one such attempt is provided in Inculet (1990). Inculet and Davenport (1994) utilized the Helmholtz resonator theory for the prediction of cavity pressure. More recently, on the basis of the Helmholtz resonator theory, Choi and Wang (1998) developed a numerical model for the prediction of cavity pressure that takes into account the flexibility of the back-panel. On the other hand, some studies (Xie *et al.* 1992, Burgess 1995, van Schijndel and Schols 1998) have been carried out to predict cavity pressure using models based on mass balance. The present study addresses the development of models, based on mass balance and the Helmholtz resonator theory, for the prediction of cavity pressure in rigid rainscreen walls.

It is important to find a way to quantify the pressure equalization performance of walls in a simple manner. This will help to compare the performance of different rainscreen walls as well as to provide a means for design. The various quantification methods can be classified based on the type of external force used in their respective formulations. Baskaran and Brown (1992) suggested a Pressure Equalization Index (PEI) to evaluate the performance of rainscreen wall assembly; Burgess (1995) introduced a Pressure Equalization Percentage (PEP) to measure the degree to which the internal joint cavity air pressure can equalize with the external air pressure fluctuations. Note that the load sharing between the rainscreen and the air barrier is not quantifiable using PEI or PEP. Further, PEI and PEP are developed to measure the cavity response under sinusoidally varying pressures at individual frequencies. In real situations, where the external wind pressures are random and non-uniform, this assumption cannot be made. It is found that the practical use of PEI and PEP is limited. In another study (van Schijndel and Schols 1998), the pressure equalization performance was quantified using a Pressure Equalization Coefficient (PEC) which is the ratio of differential pressure across the rainscreen and the differential pressure across the panel. Since the instantaneous pressure difference across the rainscreen can be higher than the pressure difference across the entire panel at the same instants (Ganguli and Dalgliesh 1988), it is inappropriate to

present the transient pressure difference across the rainscreen as a percentage of the pressure difference across the entire panel. In order to quantify the pressure equalization performance of wall systems subjected to random exterior pressure fluctuations, Xie *et al.* (1992) used rms and peak reduction factors, while Inculet (1990) used rainscreen coefficient and the peak factor for pressure drop across the rainscreen. The available quantification methods are elaborated in Suresh Kumar and van Schijndel (1998).

3. Methodology

Prediction of pressure equalization performance of rainscreen walls consists of two major steps: (1) simulation of cavity pressure and (2) quantification of pressure equalization performance. Firstly, models required for the simulation of cavity pressure are presented. Secondly, new quantification methods for assessing the performance of PER walls are suggested.

3.1. Simulation of cavity pressure

3.1.1. Model based on mass balance (Model 1)

Consider a relatively small compartmented cavity, as shown in Fig. 1. The pressure inside the cavity is assumed to be uniform. After assuming that the openings on both layers of the wall are similar and uniformly distributed, all openings on the rainscreen and on the air barrier are lumped into two groups; one group with a total area A_{rs} includes all openings on the rainscreen and the other with a total area A_{ab} includes all openings on the air barrier. The wall layers and the air flow through them are considered to be rigid and incompressible respectively.

The polytropic law relating pressure and density of air inside the cavity is

$$\frac{P_c}{\rho_c^{\beta}} = \text{constant} \tag{1}$$

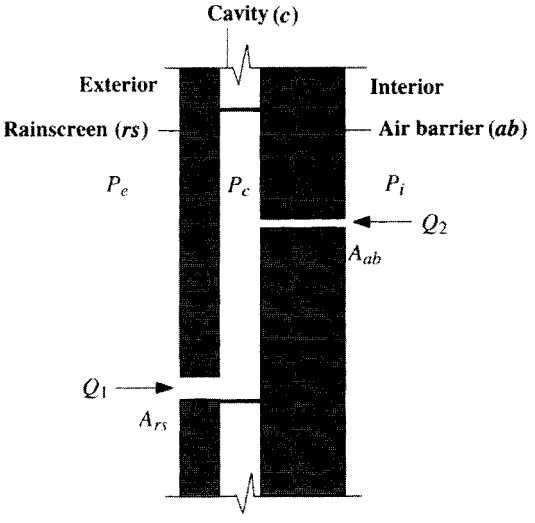

Fig. 1 Schematic of a rainscreen panel

where, P_c = cavity pressure (Pa), ρ_c = density of air inside cavity (kg/m^3), β = polytropic exponent (β = 1.0 for isothermal condition, and β = 1.4 for adiabatic condition). Differentiating Eq. (1) with respect to time (t) yields,

$$\frac{1}{P_c}\frac{dP_c}{dt} = \frac{\beta}{\rho_c}\frac{d\rho_c}{dt} \tag{2}$$

Considering Fig. 1, conservation of mass of air inside the cavity requires that the rate of net mass flows into or out the cavity must equal the rate of change of the mass of air inside the cavity (m_c) :

$$\rho_c\,(Q_1+Q_2) = \frac{dm_c}{dt} = \frac{d}{dt}(\rho_c\,V_c) = \rho_c\frac{dV_c}{dt} + V_c\frac{d\rho_c}{dt} \tag{3}$$

where, Q_1 = volumetric flow through rainscreen (m^3/s), Q_2 = volumetric flow through air barrier (m^3/s), V_c = cavity volume (m^3). After assuming the walls are not flexible, $dV_c/dt = 0$ and substitution of Eq. (2) into Eq. (3) yields,

$$(Q_1+Q_2) = \frac{V_c}{\beta P_c}\frac{dP_c}{dt} \tag{4}$$

The volumetric airflow rate through rainscreen and air barrier are expressed as

$$Q_1 = C_{w1}A_w\,(P_e - P_c)^{n1} \tag{5}$$

$$Q_2 = C_{w2}A_w\,(P_i - P_c)^{n2} \tag{6}$$

where, C_{w1} = flow coefficient for rainscreen (mPa^{-n1}/s), C_{w2} = flow coefficient for air barrier (mPa^{-n2}/s), A_w = area of wall (m^2), P_e = external pressure (Pa), P_i = internal pressure (Pa), $n1$ = flow exponent for rainscreen, $n2$ = flow exponent for air barrier. C_{w1} and C_{w2} can be expressed as:

$$C_{w1} = C_1\frac{A_{rs}}{A_w}\;;\; C_{w2} = C_2\frac{A_{ab}}{A_w} \tag{7}$$

where, C_1 = flow coefficient for rainscreen independent of venting area (mPa^{-n1}/s), C_2 = flow coefficient for air barrier independent of leakage area (mPa^{-n2}/s), A_{rs} = total area of openings on rainscreen or venting area (m^2), A_{ab} = total area of openings on air barrier or leakage area (m^2). In case of orifice flow conditions,

$$C_1 = \sqrt{\frac{2}{\rho}}\,C_{d1}\;;\; C_2 = \sqrt{\frac{2}{\rho}}\,C_{d2} \tag{8}$$

where, ρ = density of air (kg/m^3), C_{d1} = discharge coefficient for rainscreen, C_{d2} = discharge coefficient for air barrier. After substituting Eqs. (5) and (6) in Eq. (4) and including the possibility of sign change of pressures (P_e, P_c and P_i) at certain instants, the governing equation of the time varying cavity pressure can be derived as

$$\frac{dP_c}{dt} = \frac{\beta P_c}{V_c}\left[C_{w1}A_w\,\mathrm{sign}(P_e - P_c)\,|P_e - P_c|^{n1} + C_{w2}A_w\,\mathrm{sign}(P_i - P_c)\,|P_i - P_c|^{n2}\right] \tag{9}$$

where, for instance, sign (P_e - P_c) = 1 when $P_e > P_c$ and sign (P_e - P_c) = -1 when $P_e < P_c$. The cavity pressure P_c can be estimated by solving Eq. (9). This equation cannot be solved analytically. The

solution of this equation can be obtained numerically using the ordinary differential equation routine of MATLAB (1993).

3.1.2. Model based on Helmholtz resonator theory (Model 2)

The wall layers are considered to be rigid as before. The air flow through the walls is assumed to be an incompressible flow through a sharp-edged orifice. In order to include the opening on both the rainscreen and air barrier (two openings), the conventional Helmholtz resonator theory with one opening is extended. For this formulation, consider a 'plug' of air moving in and out of the opening in both rainscreen and air barrier in response to the external pressure and internal pressure changes, respectively. Considering Fig. 2, the governing equations of motion of the plugs of air through rainscreen and air barrier are:

$$\rho L_{e1}\ddot{X}_1+\frac{\rho}{2C_{d1}^2}|\dot{X}_1|\dot{X}_1=P_e-P_c \tag{10}$$

$$\rho L_{e2}\ddot{X}_2+\frac{\rho}{2C_{d2}^2}|\dot{X}_2|\dot{X}_2=P_i-P_c \tag{11}$$

where, L_{e1} and L_{e2} = effective lengths of the plugs of air through venting area and leakage area, respectively (m), X_1 and X_2 = displacements of the plugs of air through venting area and leakage area, respectively (m). The first and second terms represent the mass and damping, respectively. The damping term is non-linear (square-law). P_c on the right side represents the stiffness term. Eqs. (10) and (11) are similar to the differential equation of a single degree of freedom system with non-linear damping.

Model 1 (Eq. 9) based on mass balance is found to be applicable for walls with different flow characteristics. On the other hand, Model 2 is inherently based on a flow exponent equal to 0.5

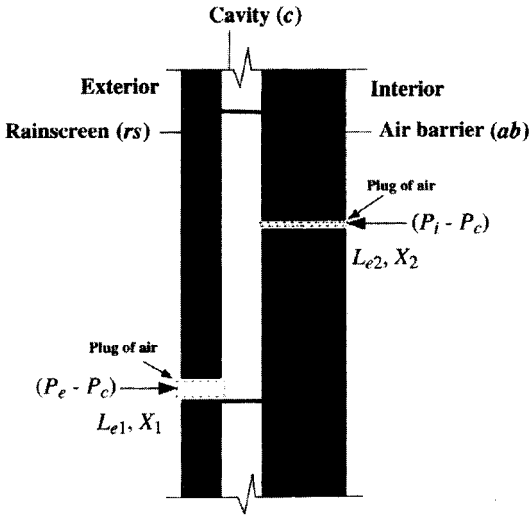

Fig. 2 Plug of air through rainscreen and air barrier

and flow coefficient equal to Eq. (8) for both rainscreen and air barrier. However, in many real cases, where the openings on the air barrier are small cracks, the flow exponent for the air barrier is found to be higher than 0.5, representing a mixture of laminar and turbulent flow cases, and the corresponding flow coefficient is different from the value obtained from Eq. (8). For instance, Tamura and Shaw (1976) have shown that the flow exponent for leakage through a building envelope may vary from 0.5 to 1.0, converging on 0.65 for buildings with HVAC systems. In these circumstances, Model 2 in its current form cannot be applied; therefore, a more general form of equations, which can be applied to different flow characteristics of rainscreen and air barrier, are required. Note that higher flow exponent can vary the damping force acting on the plug of air. Therefore, the damping term in the governing equation of motion of the plugs of air through rainscreen and air barrier (Eqs. 10 and 11) has to be modified based on general flow exponents and flow coefficients. The modified equations are of the form:

$$\rho L_{e1}\ddot{X}_1+\frac{1}{C_1^{1/n1}}\left|\dot{X}_1\right|^{\frac{1}{n1}-1}\dot{X}_1=P_e-P_c \tag{12}$$

$$\rho L_{e2}\ddot{X}_2+\frac{1}{C_2^{1/n2}}\left|\dot{X}_2\right|^{\frac{1}{n2}-1}\dot{X}_2=P_i-P_c \tag{13}$$

Eqs. (12) and (13) reduce to Eqs. (10) and (11) when $n1=n2=0.5$ and, C_1 and C_2 are provided by Eq. (8).

The mass continuity equation is expressed as:

$$\frac{dm_c}{dt}=\rho_c A_{rs}\dot{X}_1+\rho_c A_{ab}\dot{X}_2 \tag{14}$$

Substituting Eqs. (2) and (3) in Eq. (14) yields,

$$\frac{dP_c}{dt}=\frac{\beta P_c}{V_c}\left[A_{rs}\dot{X}_1+A_{ab}\dot{X}_2\right] \tag{15}$$

The cavity pressure P_c can be estimated by solving Eqs. (12), (13) and (15). They are not analytically solvable like the previous case, and so have to be solved numerically. After rewriting the second order differential equations (Eqs. 12 and 13) as a system of coupled first order differential equations, they can be solved using the ordinary differential equation routine of MATLAB (1993).

3.2. Quantification of pressure equalization performance

It has been found that it is very difficult to provide a single representation for the pressure equalization performance of walls. In this investigation, on the basis of the differential pressure across the rainscreen ($\Delta P_{rs}=P_e-P_c$) and the differential pressure across the composite panel ($\Delta P_t=P_e-P_i$), methods for the quantification of pressure equalization performance of rainscreen walls are recommended. The suggested evaluation methods are as follows: (1) Mean Pressure Equalization Coefficient (MPEC), (2) Standard deviation Pressure Equalization Coefficient (SPEC) and (3) Peak Pressure Equalization Coefficient (PPEC) :

$$\text{MPEC} = \frac{|\overline{\Delta P_{rs}}|}{|\overline{\Delta P_t}|} \; ; \; \text{SPEC} = \sqrt{\frac{\overline{[\Delta P_{rs} - \overline{\Delta P_{rs}}]^2}}{\overline{[\Delta P_t - \overline{\Delta P_t}]^2}}} \; ; \; \text{PPEC} = \frac{\max(|\Delta P_{rs}|)}{\max(|\Delta P_t|)} \tag{16}$$

In this formulation, MPEC evaluates the static pressure equalization performance, while SPEC and PPEC collectively evaluate the dynamic pressure equalization performance. The values of MPEC, SPEC and PPEC are expected to range between zero and one. Low values indicate good pressure equalization and higher values indicate poor pressure equalization. It is also possible to determine the load sharing between the wall layers using these quantification methods.

4. Comparisons between full-scale and simulation results

4.1. Full-scale measurements

For validation of the models, differential pressure measurements performed on the facade of the main building of the Technical University of Eindhoven (Suresh Kumar 1998b, Suresh Kumar and Wisse 1999) have been utilized. The field facility is located on the main building of the TUE. For this investigation, the glass cladding of a facade-element was replaced with a test panel. This wooden panel of size 1 m × 1.3 m (panel area, $A_w = 1.3$ m^2) was mounted approximately on the middle of the west side facade at a height of about 39 m above the ground. A SOLENT ultrasonic anemometer was used for the three component wind velocity

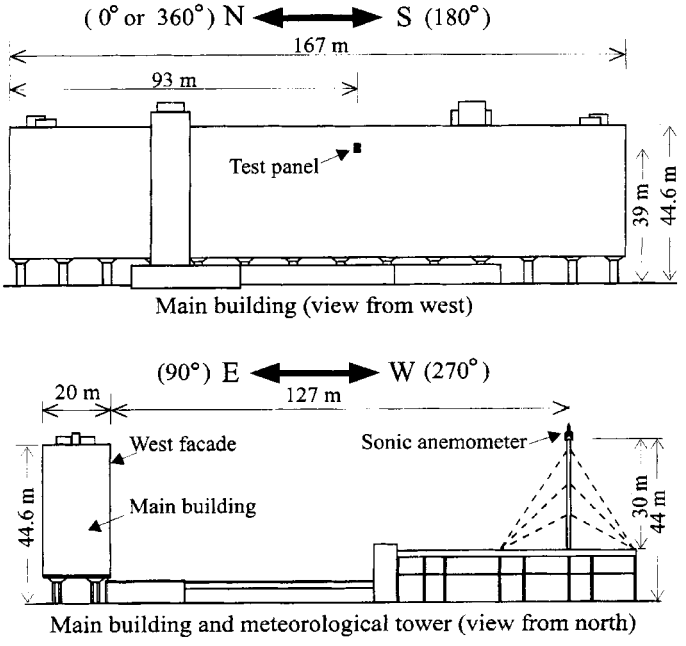

Fig. 3 Sketch of the field facility

Table 1 Details of the measurement configuration

Case	Venting	Air barrier leakage	Mean wind speed (m/s)/Mean wind direction
1	Circular holes A_{rs} = 0.001979 C_{d1} = 0.61, $n1$ = 0.5	Straw C_{ab} = 0.000314 $n2$ = 0.71	13.2, 252.1
2	Circular holes A_{rs} = 0.001979 C_{d1} = 0.61, $n1$ = 0.5	Straw C_{ab} = 0.000314 $n2$ = 0.71	7.0, 276.9
3	Circular holes A_{rs} = 0.001979 C_{d1} = 0.61, $n1$ = 0.5	Filter C_{ab} = 0.000171 $n2$ = 1.0	10.0, 252.5

Note: A_{rs} = venting area (m^2), C_{d1} = discharge coefficient of rainscreen, $n1$ = flow exponent of rainscreen, C_{ab} = flow coefficient of air barrier (mPa^{-n2}/s), $n2$ = flow exponent of air barrier.

measurements, and was mounted at the top of a 30 m high mast placed on a 14 m high building, 127 m westward of the main building of the university. Fig. 3 shows the field facility. The test panel consisted of an outer blade (rainscreen), an inner blade (air barrier) and an air space (cavity) between them; the cavity depth can be varied between 25 mm and 250 mm. The venting area of rainscreen was set as sharp-edged circular holes (3 mm diameter); the venting area can be varied by closing the holes. On the other hand, two air barrier leakage configurations had been used: (1) three sets of straws, each 15 cm long and 5 mm dia., in three circular holes (dia. 2 cm, 3.8 cm, 2 cm) at three different locations in the middle of the panel, and (2) industrial metal filter. The flow characteristics of venting and air barrier leakage reported in Table 1 had been determined using simple static pressurization tests, where flow rate and the corresponding pressure drop were measured. Four pressure taps each were installed on the rainscreen and air barrier for pressure measurements. Differential pressure transducers were used to measure external and cavity pressures with reference to internal building pressure ($P_e - P_i$ and $P_c - P_i$ respectively). In each run, the exterior and cavity pressure data were simultaneously measured at four taps each at a sampling rate of 20 Hz for 10 minutes. The velocity data were also acquired by the same data acquisition system (PhyDAS) at a rate of 20.83 Hz. The data acquisition was controlled by the mean wind velocity measurements; the data acquisition was triggered when the mean wind velocity in the last minute exceeds a preset value (6 m/s). In the analysis, for each run, representative differential pressure time series across the panel ($P_e - P_i$) and across the air barrier ($P_c - P_i$) were calculated by respectively averaging the measurements at four exterior taps and at four cavity taps. Later on, these averaged pressure records were analyzed in time, frequency and amplitude domains. Measurement details can be found in Suresh Kumar and Wisse (1999).

For demonstration purposes, three typical measurements have been chosen for which V_c = 0.195 m^3. Table 1 shows the details of the experimental configurations including the mean wind speeds and directions at mast height. Note that wind direction 270° represents wind blowing perpendicular to the west side of the building where the panel and the meteorological tower are located. Fig. 4 shows the measured differential pressure across the panel for the three cases. These time histories have been used as inputs in the simulations. Table 2 shows the statistics of the

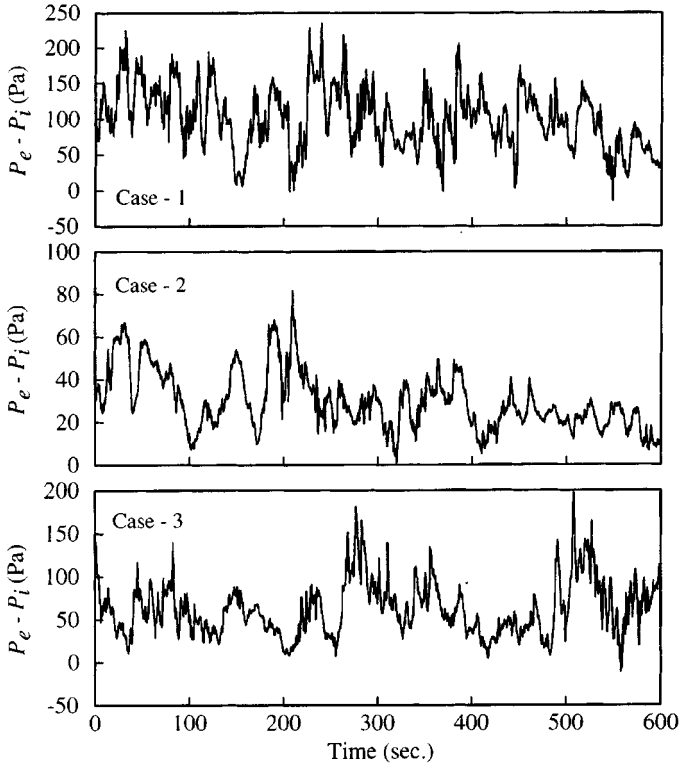

Fig. 4 Sample measured differential pressure time histories across the panel

Table 2 Statistics of measured data

		Case-1 (Pa)	Case-2 (Pa)	Case-3 (Pa)
$P_e - P_i$	mean	100.53	29.65	62.12
	rms	42.60	13.68	31.46
	peak	234.94	81.69	197.26
$P_c - P_i$	mean	62.51	17.84	23.55
	rms	27.06	9.38	13.23
	peak	146.34	51.95	70.64
$P_e - P_c$	mean	38.02	11.81	38.57
	rms	16.05	4.43	18.54
	peak	101.57	31.01	130.74

measured data. In general, the differential pressure across the air barrier is found to be smoother than the differential pressure across the panel and as a result, the corresponding rms pressures across the air barrier are generally lower than those across the panel. This shows that the higher frequency panel pressures are attenuated in the cavity, signifying that the higher frequency panel pressures are transmitted to the rainscreen (Suresh Kumar 1998b). All configurations exhibit very little pressure equalization of high frequency wind gusts (Suresh Kumar and Wisse 1999).

Comparing case 3 with cases 1 and 2, the venting areas are same; however, the leakage characteristics are quite different (see Table 1). Using a simple mass balance equation connecting airflow into the cavity with the airflow out of the cavity (Suresh Kumar 1998a, 2000), it can be easily shown that the configuration corresponding to cases 1 and 2 is more effective than case 3 in equalizing cavity pressure with the external pressure. This is clear from Table 2, where the amount of load shared by the rainscreen is much higher in case 3 compared to the other cases.

4.2. Computer simulations

The polytropic exponent, β, is 1.0 for isothermal condition; however, when the pressure and density changes inside the cavity are rapid, the process inside the cavity can be considered as adiabatic, in which case $\beta = 1.4$ should be used. Considering the lack of knowledge in this issue, an intermediate value of 1.2 is used in the simulations; this value is also used by Holmes (1979) in computing wind-induced pressures inside buildings. Further, in the simulations L_{e1} and L_{e2} can be taken to be $\sqrt{\pi A_{rs}/4}$ and $\sqrt{\pi A_{ab}/4}$, respectively; this is correct for circular openings and is a good approximation for rectangular openings as well (Malecki 1969). The time varying cavity pressure P_c has been simulated using Models 1 and 2; these simulations employ $\rho = 1.23$ Kg/m^3, $\beta = 1.2$, the measured differential pressure across the panel, $P_e - P_i$ (shown in Fig. 4), and the flow characteristics of rainscreen and air barrier (shown in Table 1). Since all the external and cavity pressure measurements are made with reference to the internal building pressure (P_i), the value of P_i is not known. For computation purposes, P_i is assumed to be equal to the atmospheric pressure, $P_o = 10^5$ Pa; this will not alter the final results since they are based on differential pressures across rainscreen, air barrier and panel by deducting P_i from corresponding pressures. In computation, the initial condition of P_c is chosen as the sum of the first data point of $P_e - P_i$ and P_o. Because of this, the simulation will take about four data points to become stable and therefore, the simulated results are based on time series without the first four data points.

4.2.1. Performance of Model 1 and Model 2

Fig. 5 shows the differential pressures across the rainscreen simulated by Models 1 and 2. The first minute of the time history of case 1 has been used as the input in these simulations. The corresponding simulated time histories by Model 1 and 2 are in agreement with each other. Further, Table 3 shows good agreement between the simulations using the suggested quantification methods. The same results have been noted in many diverse cases.

On the other hand, for an enclosed cavity with only openings on the rainscreen and zero air barrier leakage ($A_{ab} = 0$), the undamped natural frequency of the system, f, in Hz can be derived using Eqs. (12) and (15) as:

$$f = \frac{1}{2\pi}\sqrt{\frac{\beta A_{rs} P_c}{\rho L_{e1} V_c}} \tag{17}$$

Since the order of variation of P_c above and below P_o is negligible compared to the value of P_o, P_c can be assigned the value of P_o; therefore, this assumption would not significantly alter the estimated value of frequency. Substituting $\beta = 1.2$, $P_c = P_o = 10^5$ Pa, $\rho = 1.23$ Kg/m^3, L_{e1}

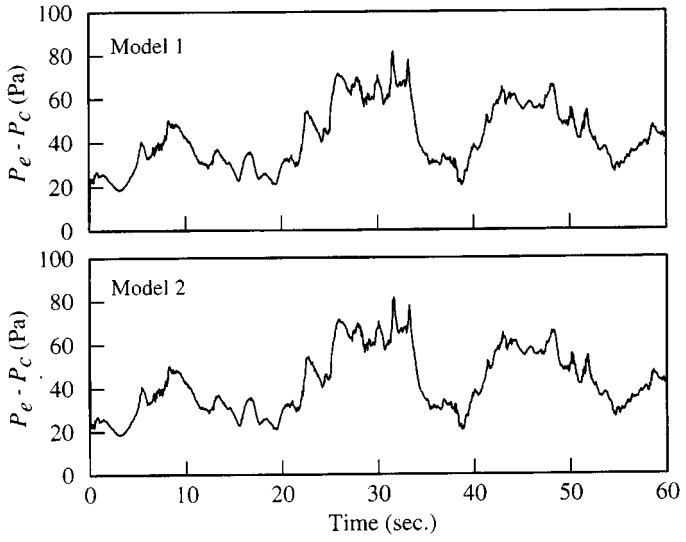

Fig. 5 Simulated pressure time histories using Models 1 and 2

Table 3 Simulation results using Models 1 and 2

	Model 1	Model 2
MPEC	0.32	0.32
SPEC	0.40	0.40
PPEC	0.36	0.36

$= \sqrt{\pi A_{rs}/4}$ in Eq. (17) and rearranging the terms yields,

$$f \approx 52.8 \left(\frac{A_{rs}^{1/4}}{V_c^{1/2}} \right) \approx 52.8 \frac{(A_{rs}/A_w)^{1/4}}{d_c^{1/2} A_w^{1/4}} \tag{18}$$

where, the factor 52.8 has dimensions (m/s), d_c is the cavity depth (m). As far as the resonance is concerned, it is of particular interest to show when the system frequency is close to the frequencies of the external pressures (the major portion of the wind pressure spectrum lies between 0.1 Hz and 2 Hz - see Suresh Kumar 1998b). Low system frequency (f) can be achieved for a combination of small A_{rs}/A_w and large d_c. Considering a relatively worst case scenario with $A_{rs}/A_w = 0.0025$, $A_w = 25$ m^2 and $d_c = 0.2$ m, the estimated $f \approx 12$ Hz is much higher than the frequencies of major external pressures. Note that usually in practice, the value of A_{rs}/A_w will be higher and the value of A_w and d_c will be lower than those chosen for this estimation. As a result, in general, the system frequency, f, is between 50 and 150 Hz. Therefore, any resonance arising from the inertial term of Eq. (12) lies well into the high frequency tail of the external pressure spectrum and thus is unlikely to be excited to any significant amplitude. These simple calculations show that the inertial term can be avoided in the formulation of Model 2. Model 2 becomes Model 1 without the inertial term. The similarity between the results of Model 1 and Model 2 indicate the triviality of the inertial term in Model 2.

Note also that the simulation using Model 1 is much faster than that using Model 2. For instance, in the case of Fig. 5, the number of floating point operations have been counted which are respectively 1.1×10^8 and 2.7×10^9 for simulation using Model 1 and 2; for this small input time history of 1 minute, the number of operations in the simulation using Model 2 is approximately 25 times higher than those in the simulation using Model 1. Based on this discussion, it is realized that Model 1 is adequate and efficient for the prediction of cavity pressure and therefore, it has been proposed for carrying out parametric studies. Here onwards, all the simulations have been performed using Model 1.

4.2.2. Influence of β on simulation results

In order to comprehend the influence of the value of β on simulation results, three simulations have been performed with $\beta = 1.0$, 1.2 and 1.4 for case 1. The simulation results provided in Table 4 show the negligible influence of β on the simulation results. The rest of the simulations have been performed using the intermediate value of 1.2.

4.2.3. Comparing simulations with measurements

Figs. 6, 7 and 8 show the measured and simulated rainscreen pressures for all three cases. The simulated pressures are in close agreement with the corresponding measured pressures. Though there is no apparent difference between the simulated and measured time histories, a closer look at the results reveals that the simulated time histories are smoother and the associated peaks are somewhat underpredicted. To illustrate these points more clearly, the normalized power spectral density functions ($S(f)/\sigma^2$) of the simulated and measured differential pressures across the rainscreen are shown in Fig. 9. The comparison of the spectra appears satisfactory. However, the higher amplitudes of the spectra of the measured rainscreen pressures compared to those of the simulated rainscreen pressures for frequencies above 1 Hz reveal that a smaller percentage of high frequency fluctuations are transferred to the rainscreen in the case of simulations compared to the measurements. Table 5 shows the statistics of the simulated and corresponding measured data. Note that all these cases correspond to windward wall for relatively high turbulence levels (rms of $(P_e - P_i)$/mean of $(P_e - P_i) \sim 0.4$ to 0.5). In all three cases, the full-scale data indicates a higher mean pressure drop across the rainscreen compared to the simulation. Though this is unexplained, this observation is in general agreement with that of Inculet (1990), who also found that their theory underestimates the mean pressure drop across the rainscreen compared to the

Table 4 Statistics of simulated data using different polytropic exponents

		$\beta = 1.0$ (Pa)	$\beta = 1.2$ (Pa)	$\beta = 1.4$ (Pa)
$P_c - P_i$	mean	69.9212	69.9214	69.9216
	rms	26.9042	26.9050	26.9056
	peak	149.1297	149.1296	149.1300
$P_c - P_c$	mean	30.6163	30.6161	30.6160
	rms	15.7693	15.7673	15.7660
	peak	85.8898	85.8542	85.8423

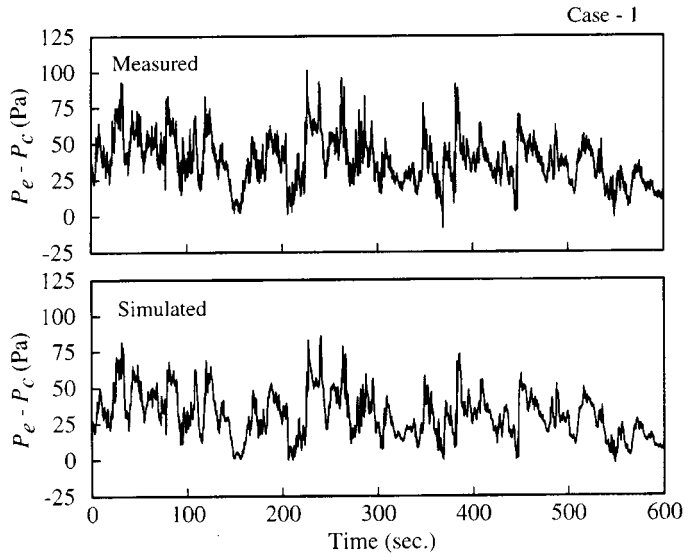

Fig. 6 Comparison of measured and simulated rainscreen pressures (Case 1)

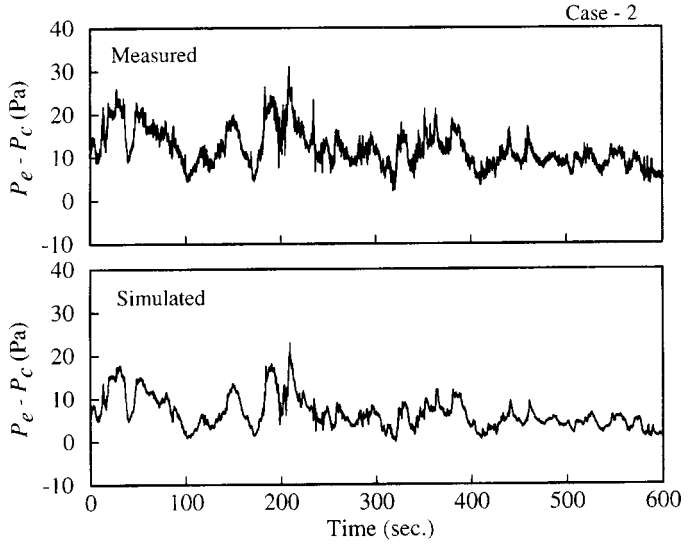

Fig. 7 Comparison of measured and simulated rainscreen pressures (Case 2)

wind tunnel data for windward wall cases under high turbulence. In general, the statistics of the simulated differential pressure across the rainscreen are lower than those of the measured cases. The underprediction of the rainscreen pressures is a result of the over prediction of the cavity pressure as shown in Table 5. Furthermore, Table 6 shows the comparison of the simulation with the measurement results using MPEC, SPEC and PPEC. In general, these are underpredicted in simulations, particularly, the MPEC and PPEC values.

Fig. 10 shows the comparison between the simulation and measurement in terms of extreme differential pressures across the rainscreen. In this analysis, extreme positive rainscreen pressure

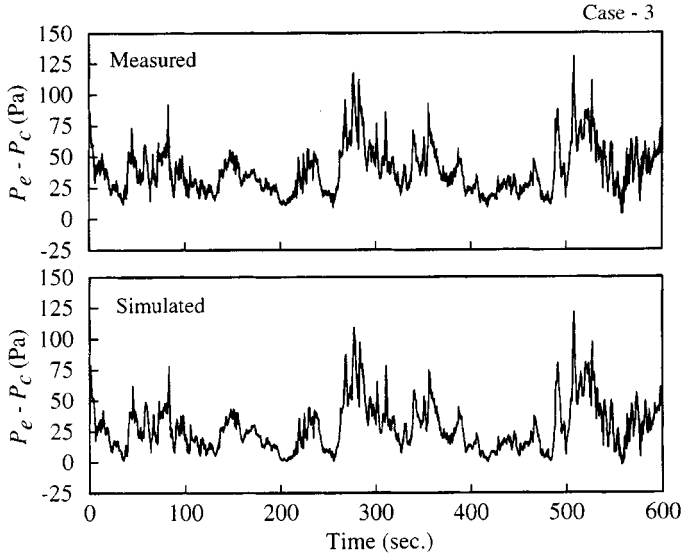

Fig. 8 Comparison of measured and simulated rainscreen pressures (Case 3)

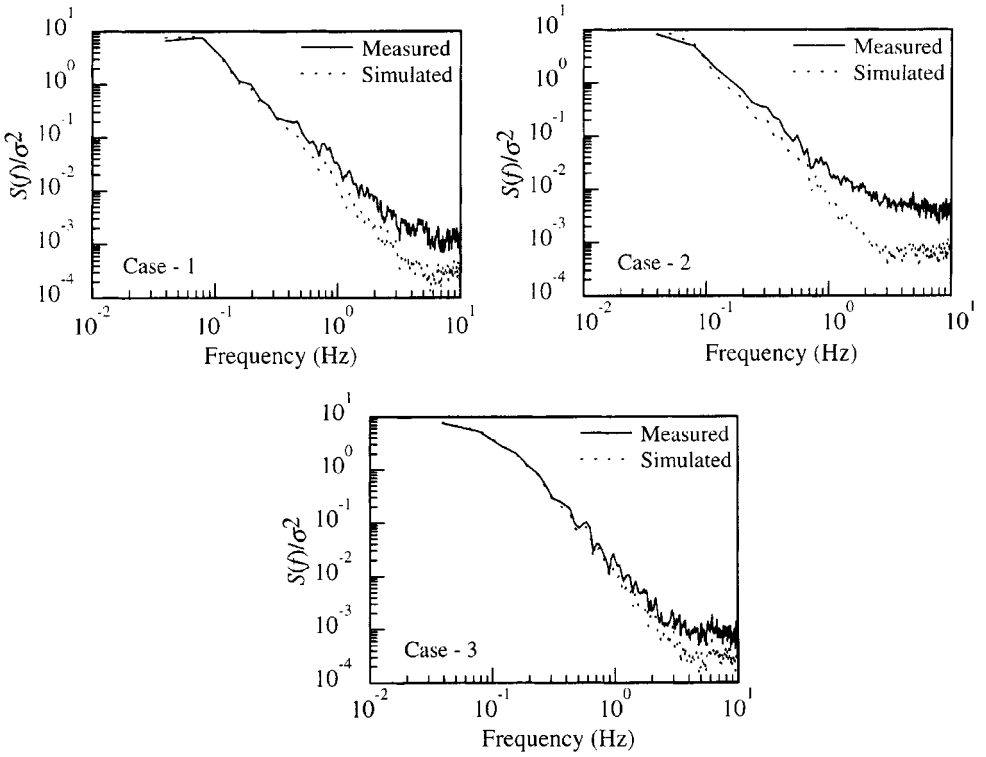

Fig. 9 Comparison of spectra of measured and simulated rainscreen pressures

$(P_e - P_c)$ values are obtained as follows: the 12000 measured as well as simulated rainscreen pressures are divided into 20 segments of 600 values each (30 sec. time series) and the peak

Table 5 Statistics of simulated and corresponding measured data

		Case - 1 (Pa)		Case - 2 (Pa)		Case - 3 (Pa)	
		M	S	M	S	M	S
$P_c - P_i$	mean	62.5	69.9	17.8	23.2	23.6	34.3
	rms	27.1	26.9	9.4	9.8	13.2	12.5
	peak	146.3	149.1	52.0	58.7	70.6	76.2
$P_e - P_c$	mean	38.0	30.6	11.8	6.4	38.6	27.8
	rms	16.1	15.8	4.4	3.9	18.5	19.2
	peak	101.6	85.9	31.0	23.0	130.7	121.1

Note : M = Measurement, S = Simulation

Table 6 Comparison of simulated data with measured data

	Case - 1		Case - 2		Case - 3	
	M	S	M	S	M	S
MPEC	0.38	0.30	0.40	0.22	0.62	0.45
SPEC	0.38	0.37	0.32	0.28	0.59	0.61
PPEC	0.43	0.37	0.38	0.28	0.66	0.61

Note : M = Measurement, S = Simulation

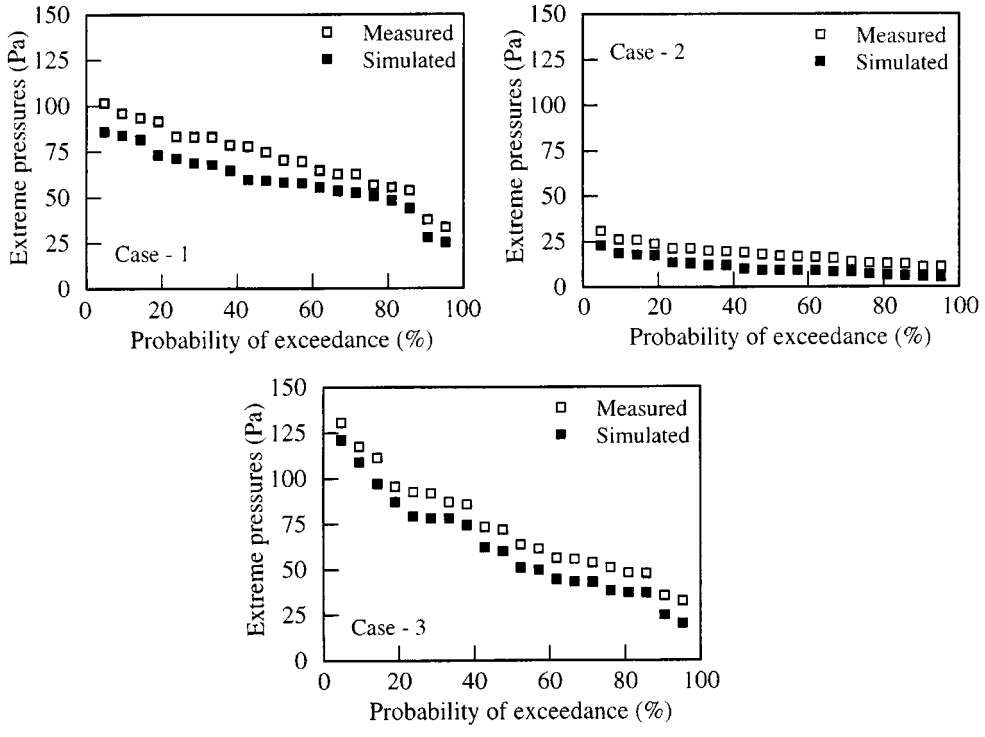

Fig. 10 Comparison of measured and simulated extreme rainscreen pressures

value from each segment is selected and plotted against the relevant risk level. Note that

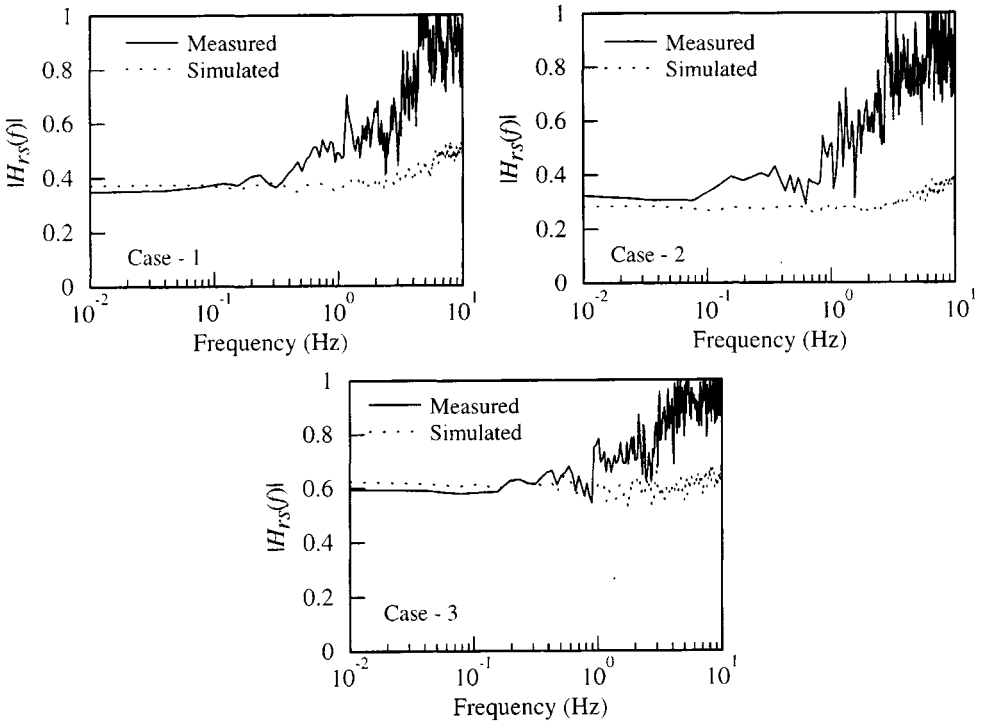

Fig. 11 Comparison of measured and simulated rainscreen pressures using transfer functions

simulation underpredicts extreme rainscreen pressures, which is expected from earlier discussions; differences up to -20% have been observed in some cases. It should be noted that these are representative results of the several simulations and comparisons performed during this investigation.

An interesting frequency domain method of analysis, estimation of transfer function has been carried out in order to relate the input (differential pressure across the panel) and the output (differential pressure across the rainscreen) of a PER facade system (Suresh Kumar and Wisse 1999). The magnitude of the transfer function for the measured and simulated differential pressure across the rainscreen ($|H_{rs}(f)|$) is shown in Fig. 11 for all the three cases. The ordinates represent measures of the ratio of wind pressure acting on rainscreen as a function of frequency; value zero indicates no pressure acting on the rainscreen, i.e. full pressure equalization occurred. In all measured cases, the magnitude of the transfer function rises rapidly after about 1 Hz. This confirms the poor performance of the configurations to equalize higher frequency fluctuations and consequently, these fluctuations are transmitted to the rainscreen. Pressure attenuation in the cavity, resulting in poor pressure equalization performance, is mainly caused by spatial pressure variations and damping of flow through the vents and in the cavity. Note that the magnitudes of the transfer functions in simulated cases are underpredicted, especially at higher frequencies. This is an expected result of the over prediction of the cavity pressures as previously discussed.

5. Discussion

The observed difference between the simulated and measured values may be due to the incorrect assumptions used in modeling. Note that the proposed model does not take into account the spatial non-uniformity of pressures acting on a panel and the appropriate damping of flow through the vents and the cavity; instead, it uses the average exterior pressures acting on the panel as a single input and the damping of flow through a single vent hole. Considering these drawbacks of the current model, the comparisons between the simulated and measured values are satisfactory. Further, there are ongoing discussions about the variation of discharge coefficients of flow through orifices under different external flow conditions (Vickery and Karakatsanis 1989, Yamaguchi 1976); the discharge coefficient is a function of the geometry of the orifice and the Reynolds number. As compared to steady flow, the value of discharge coefficient of venting is found to be significantly lower for fluctuating reversing flow and unidirectional oscillating flow conditions (Inculet 1990); during this computation, the discharge coefficient of venting was adjusted until the theoretical rms of the pressure drop across the rainscreen matched the experimental value. Previously, Holmes (1979) used a low discharge coefficient of 0.15 to achieve a reasonable agreement between the simulated and measured internal pressure spectra. Similar exercise has been carried out in this study for case 1. For instance, the C_{d1} value was lowered to 0.49 from the steady flow value of 0.61 in order to achieve the measured mean differential pressure across the rainscreen. The results are shown in Fig. 12. Note that in case of $C_{d1} = 0.61$, the transfer function magnitudes at lower frequencies are slightly over predicted and those at higher frequencies are significantly underpredicted; the SPEC value is almost matching though the MPEC and PPEC values are underpredicted as shown in Table 7. When $C_{d1} = 0.49$, the simulated MPEC value is matching with the measurement, but the SPEC and PPEC values are over predicted. It is clear that the transfer function magnitudes at lower frequencies are significantly over predicted when C_{d1} becomes 0.49, though the difference between the measured and simulated transfer function magnitudes at higher frequencies is reduced

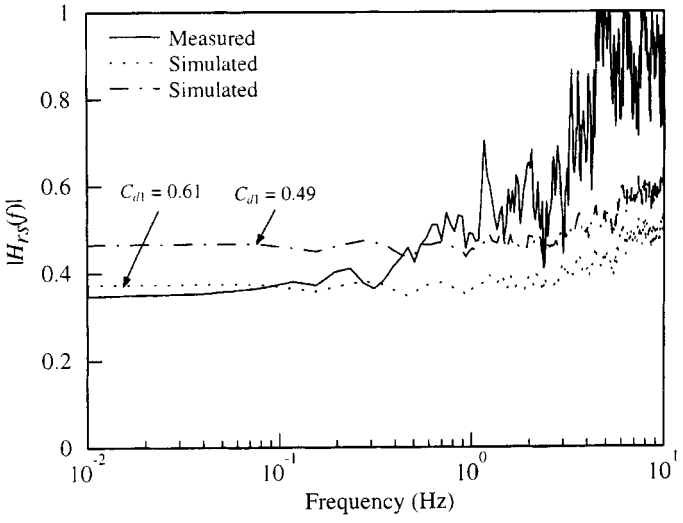

Fig. 12 The effect of discharge coefficients on rainscreen pressures

Table 7 Comparison of the results for different discharge coefficients

	Measured	$C_{d1} = 0.61$	$C_{d1} = 0.49$
MPEC	0.38	0.30	0.39
SPEC	0.38	0.37	0.46
PPEC	0.43	0.37	0.46

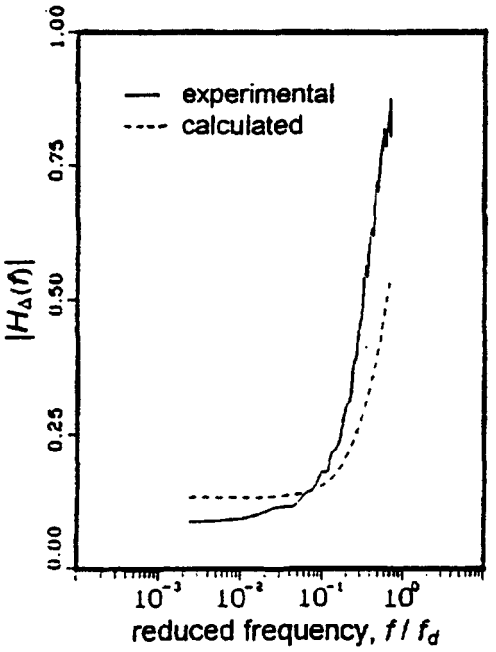

Fig. 13 Comparison of measured and simulated transfer functions for rainscreen pressures, after Inculet and Davenport (1994)

compared to the case of $C_{d1} = 0.61$. Similar results are also obtained by Inculet and Davenport (1994); a typical result of their study is shown in Fig. 13 where, $|H_\Delta(f)|$ is the magnitude of the transfer function for pressures across the rainscreen, f is the frequency and f_d is the critical damping frequency. This case corresponds to the windward wall with $A_{rs} = 13.9$ mm^2, $V_c = 413$ cm^3, $A_{ab}/A_{rs} = 0.23$; for the computation, $C_{d1} = 0.19$ was used. They claimed the discrepancy between the experimental and computed transfer functions as a result of the linearization of the damping term in their model.

When the air barrier is not leaky, the transfer function magnitudes at lower frequencies will be close to zero. In this case, by lowering the discharge coefficient can bring the transfer function magnitudes at high frequencies close to the measured without changing the magnitudes at low frequency end. Therefore, better comparison of the transfer functions is expected in case of no leakage situation by using low discharge coefficient in simulations. From Eq. (10), note that as the discharge coefficient reduces, the damping coefficient increases and as a result, the cavity pressure reduces; but the increment in damping coefficient is constant for all frequencies of fluctuations. On the other hand, the damping is suspected to be frequency dependent; probably, a

frequency dependent variation of the discharge coefficient may be required for the accurate modeling of the damping term. Further, the spatial non-uniformity of the flow across the panel can induce poor pressure equalization performance. Since an averaged pressure across the panel is used as input in simulations, the simulated cavity pressures are higher than the measured values which is the case here. In short, the spatial non-uniformity of the flow as well as the damping of flow through the vents has to be investigated further in order to incorporate these effects in the modeling procedure.

Regardless of these limitations, the proposed model is an efficient tool to investigate the influence of various parameters on pressure equalization performance, which is otherwise time consuming and difficult using full-scale tests. Currently, efforts are directed to extend the computer model to account for spatial non-uniformity of external flow as well as appropriate damping of flow through vents. More field measurements will be carried out for comprehensive comparison of simulated results with the measurements as well as for quantifying the uncertainties involved in the prediction.

6. Conclusions

This paper is concerned primarily with the theoretical prediction of pressure equalization performance of rigid rainscreen walls. The time varying cavity pressure has been simulated using models based on mass balance and on the Helmholtz resonator theory. Thereafter, the proposed evaluation methods have been utilized to assess the pressure equalization performance of rainscreen walls. The results clearly show that the model based on mass balance is sufficiently accurate and efficient compared to the other, and is adequate for a parametric study of cavity pressure dynamics. For the first time, the model performance is validated using full-scale data. The results based on the proposed model show reasonably good agreement with those obtained from full-scale tests. Possible reasons for the underprediction of rainscreen pressures at higher frequencies are also discussed.

Acknowledgements

The authors thank the reviewers for providing useful comments and suggestions to improve the manuscript. The authors also acknowledge the valuable suggestions of Dr. T. Stathopoulos of Concordia University, Montreal, Canada.

References

Baskaran, B.A. and Brown, W.C. (1992), "Performance of pressure equalized rainscreen walls under cyclic loading", *J. Thermal Insul. and Bldg. Envs.*, **16**, 183-193.

Burgess, J.C. (1995), "Pressure equalized rainscreen joint modelling with numerical model PERAM", *Bldg. Envir.*, **30**(3), 385-389.

Choi, E.C.C. and Wang, Z. (1998), "Study on pressure-equalization of curtain wall systems", *J. Wind Eng. Ind. Aerodyn.*, **73**, 251-266.

Fazio, P. and Kontopidis, T. (1988), "Cavity pressure in rain screen walls", *Bldg. Envir.*, **23**(2), 137-143.

Ganguli, U. and Dalgliesh, W.A. (1988), "Wind pressures on open rain screen walls: Place Air Canada", *J. Struct. Eng., ASCE*, **114**(3), 642-656.

Holmes, J.D. (1979), "Mean and fluctuating internal pressures induced by wind", Proc *roceedings of the 5th International Conference on Wind Engineering*, Boulder, Colorado, 1979.
Inculet, D.R. (1990), "Pressure-equalization of rainscreen cladding", M.E.Sc. Thesis, Faculty of Engineering Science, The University of Western Ontario, Canada.
Inculet, D.R. and Davenport, A.G. (1994), "Pressure-equalized rainscreens: A study in the frequency domain", *J. Wind Eng. Ind. Aerodyn.*, **53**, 63-87.
Kerr, D.D. (1985), "Annotated bibliography on the rain screen principle", *Division of Building Research, Bibliography*, **45**, (613) 993-2463, NRCC, Ottawa.
Killip, I.R. and Cheetham, D.W. (1984), "The prevention of rain penetration through external walls and joints by means of pressure equalization", *Bldg. Envir.*, **19**(2), 81-91.
Latta, J.K. (1973). *Walls, windows and roofs for the Canadian climate - a summary of the current basis for selection and design*, Special Technical Publication No. 1 , NRCC 13487, National Research Council of Canada, Ottawa.
Malecki, I. (1969). *Physical Foundations of Technical Acoustics*, Pergamon Press, Oxford.
MATLAB (1993). *User's Guide*, The MathWorks Inc., Massachusetts.
Suresh Kumar, K. (2000), "Pressure equalization of rainscreen walls: A critical review", *Bldg. Envir.*, **35**(2), 161-179.
Suresh Kumar, K. (1998a), "Pressure equalized rainscreen approach to wall design: Past accomplishments and future challenges", Report: FAGO 98.25.K, Faculty of Architecture, Building and Planning, Technical University of Eindhoven, The Netherlands.
Suresh Kumar, K. (1998b), "Pressure equalization performance of rainscreen walls: Experimental investigations", *Proceedings of the 2nd East European Conference on Wind Engineering*, Prague, Czech Republic, September.
Suresh Kumar, K. and van Schijndel, A.W.M. (1998), "Cavity pressure dynamics of rainscreen walls", *Proceedings of the 4th UK Conference on Wind Engineering*, Bristol, UK, September.
Suresh Kumar, K. and Wisse, J.A. (1999). "A full-scale study on pressure equalization of rainscreen facades", *Proceedings of the 10th International Conference on Wind Engineering*, Copenhagen, Denmark, June.
Tamura, G.T. and Shaw, C.Y. (1976), "Studies on exterior wall air tightness and air infiltration of tall buildings", *ASHRAE Transactions*, **82**(Part I), 122-134.
van Schijndel, A.W.M. and Schols, S.F.C. (1998), "Modeling pressure equalization in cavities", *J. Wind Eng. Ind. Aerodyn.*, **74-76**, 641-649.
Vickery, B.J. and Karakatsanis, C. (1989), "Discharge coefficients and internal pressures in well ventilated buildings", *Proceedings of the 2nd Asia-Pacific Symposium on Wind Engineering*, Beijing, China.
Xie, J., Schuyler, G.D. and Resar, H.R. (1992), "Prediction of net pressure on pressure equalized cavities", *J. Wind Eng. Ind. Aerodyn.*, **41-44**, 2449-2460.
Yamaguchi, A. (1976), "Non-steady characteristics of orifices", *Bulletin of the JSME*, 1976, **19**(131), 505-512.

Notations

A_{ab}	total area of openings on air barrier or leakage area (m^2)
A_{rs}	total area of openings on rainscreen or venting area (m^2)
A_w	area of wall (m^2)
β	polytropic exponent
C_1	flow coefficient for rainscreen independent of venting area (mPa^{-n1}/s)
C_2	flow coefficient for air barrier independent of leakage area (mPa^{-n2}/s)
C_{d1}	discharge coefficient for rainscreen
C_{d2}	discharge coefficient for air barrier

C_{w1}	flow coefficient for rainscreen (mPa^{-n1}/s)
C_{w2}	flow coefficient for air barrier (mPa^{-n2}/s)
d_c	cavity depth (m)
ΔP_{rs}	differential pressure across the rainscreen (Pa)
ΔP_t	differential pressure across the composite panel (Pa)
f	undamped natural frequency of the system (Hz)
$\|H_{rs}(f)\|$	magnitude of the transfer function for differential pressure across rainscreen
L_{e1}	effective length of plug of air through venting area (m) $= \sqrt{\pi A_{rs}/4}$
L_{e2}	effective length of plug of air through leakage area (m) $= \sqrt{\pi A_{ab}/4}$
m_c	mass of air inside the cavity (kg)
n_1	flow exponent for rainscreen
n_2	flow exponent for air barrier
P_c	cavity pressure (Pa)
P_e	external pressure (Pa)
P_i	internal pressure (Pa)
P_o	atmospheric pressure (Pa)
Q_1	volumetric flow through rainscreen (m^3/s)
Q_2	volumetric flow through air barrier (m^3/s)
ρ	density of air (kg/m^3)
ρ_c	density of air inside cavity (kg/m^3)
$S(f)$	spectral density function
V_c	cavity volume (m^3)
X_1	displacement of plug of air through venting area (m)
X_2	displacement of plug of air through leakage area (m)

(*Communicated by Giovanni Solari*)